Swiss J Geosci (2010) 103:43–59
DOI 10.1007/s00015-010-0001-9

Rossberg landslide history and flood chronology as recorded in Lake Lauerz sediments (Central Switzerland)

Felix Bussmann · Flavio S. Anselmetti

Received: 5 March 2009 / Accepted: 29 January 2010 / Published online: 28 May 2010

Abstract The southern slopes of Rossberg mountain, Central Switzerland, on which one of the largest historic landslides of the Alpine region was released in 1806 AD (Goldauer Bergsturz), are prone to large-scale mass wasting processes. This has led to numerous sliding events, which are well-recognizable in the modern topography but lack accurate dating. In order to provide new insights into the timing and the processes associated with past landslides as well as into the frequency of exceptional flood events, long sediment cores were retrieved from the subsurface of Lake Lauerz that lies in the pathway of these landslides and that records strong runoff events with typical flood layers. Analyses of the recovered cores display a sedimentologic succession with variable fingerprints of past landslides and flood events, depending on the coring location within the lake. The landslide signature can be calibrated using the 1806 AD event: An organic-rich peaty unit, which is found in two cores located close to the rockmass impact, points towards a sudden, gravity spreading-induced lateral displacement of the swampy plain where parts of the rock mass were accumulating. This rapid lateral mobilization of soft sediments, and not the rock masses, acted as ultimate trigger for the reported ~15 m-high impulse waves on the lake. In the more distal areas, the 1806 AD event led to the deposition of a thick, organic-rich redeposited layer. The 10 m-long core from the distal basin covers a radiocarbon-dated ~2,000 years sedimentation history and contains a highly similar event layer that was deposited in 810 ± 60 AD. This layer is most likely the product of a major historic landslide, known as Röthener Bergsturz, which, based on scarce historical reports, was commonly dated to 1222 AD. In the 2,000 years record, we identify three periods with enhanced occurrence of flood turbidites dated to 580–850 AD, 990–1420 AD, and 1630–1940 AD. Among the 54 detected flood layers, 6 probably mark exceptionally heavy rainfall events that are dated to ~610, ~1160, ~1290, ~1660, ~1850, and ~1876 AD, the latter being associated to one of the most intense rainfall events ever recorded instrumentally in the region.

Keywords Lauerz · Goldau · Lake sediments · Rock avalanche · Landslide succession · Impulse wave · Gravity spreading · Flood events

Introduction

Mass movements are common features in mountainous regions. They represent an important landscape-forming factor, are a considerable hazard and cause major disasters on a global scale every year (Nadim et al. 2006). Additionally, if the sliding mass falls into a water body or is released on subaqueous slopes, they can cause catastrophic waves, comparable with marine tsunamis (Fritz et al. 2001, 2004; Fritz 2002; Schnellmann et al. 2002, 2005; Bardet et al. 2003). These waves can cause disaster due to run-up along the shoreline and overtopping of dams (Vischer and Hager 1998). The Lituya Bay rockslide impact, as an example, is probably the most prominent event for this

Editorial handling: H. Weissert and A. G. Milnes.

F. Bussmann
Department of Earth Sciences, Geological Institute, ETH Zürich, Zürich, Switzerland
e-mail: bussmannfelix@gmail.com

F. S. Anselmetti (✉)
Eawag, Swiss Federal Institute of Aquatic Science and Technology, Department of Surface Waters, Dübendorf, Switzerland
e-mail: flavio.anselmetti@eawag.ch

kind of natural disaster: In 1958, an 8.3 magnitude earthquake triggered a major subaerial rockslide into the bay of Lituya, Alaska. The sliding mass impacted the water at high speed, which resulted in the largest impulse wave run-up of 524 m ever recorded in history (Fritz et al. 2001).

On 2 September 1806 AD, a huge rock mass was released on the slopes of Rossberg mountain, Central Switzerland, referred to as 'Rossberg slide' or 'Goldauer Bergsturz' (Fig. 1). The rock avalanche claimed 457 victims and destroyed almost the entire former village of Goldau (Zay 1807; Heim 1932; Zehnder 1988). Additionally, it is reported that the easternmost part of the sliding mass hit Lake Lauerz, triggering devastating water waves of ~15 m height and reducing the lake's superficial area by at least 1/7 of its original size. Around ten people died in the resulting flood on the southern shores of the lake (Zay 1807; Zehnder 1988).

The Rossberg slide, which involved approximately 36 million m^3 of rock (Berner 2004; Thuro et al. 2006) is known as one of the major historic landslides in the alpine region and was therefore investigated by numerous geologists (e.g. Heim 1932; Kopp 1936; Lehmann 1942; Berner 2004; Thuro et al. 2006). Results of these studies reveal that the 1806 AD event was not the only mass wasting event emanating from the slopes of Rossberg mountain but rather the preliminary terminus of an ongoing landslide succession. Kopp (1936) identified around 20 mostly prehistoric mass wasting events through field observations of slide scars and mass movement deposits, whereof the 1806 AD rock avalanche was not even the biggest event. A more recent study confirms that besides the 1806 AD sliding plane, several other sliding planes can be recognized in the field (Berner 2004; Thuro et al. 2006). In addition to the 1806 AD event, three major mass movements are reported in the literature, whereof one event took place in historic times (Fig. 1). This historic slide, referred to as 'Röthener Bergsturz', which destroyed the former village of Röthen, is believed to have occurred in 1222 AD or before 1354 AD respectively, depending on the historic document cited (Zay 1807; Dettling 1860). The other two major precursors

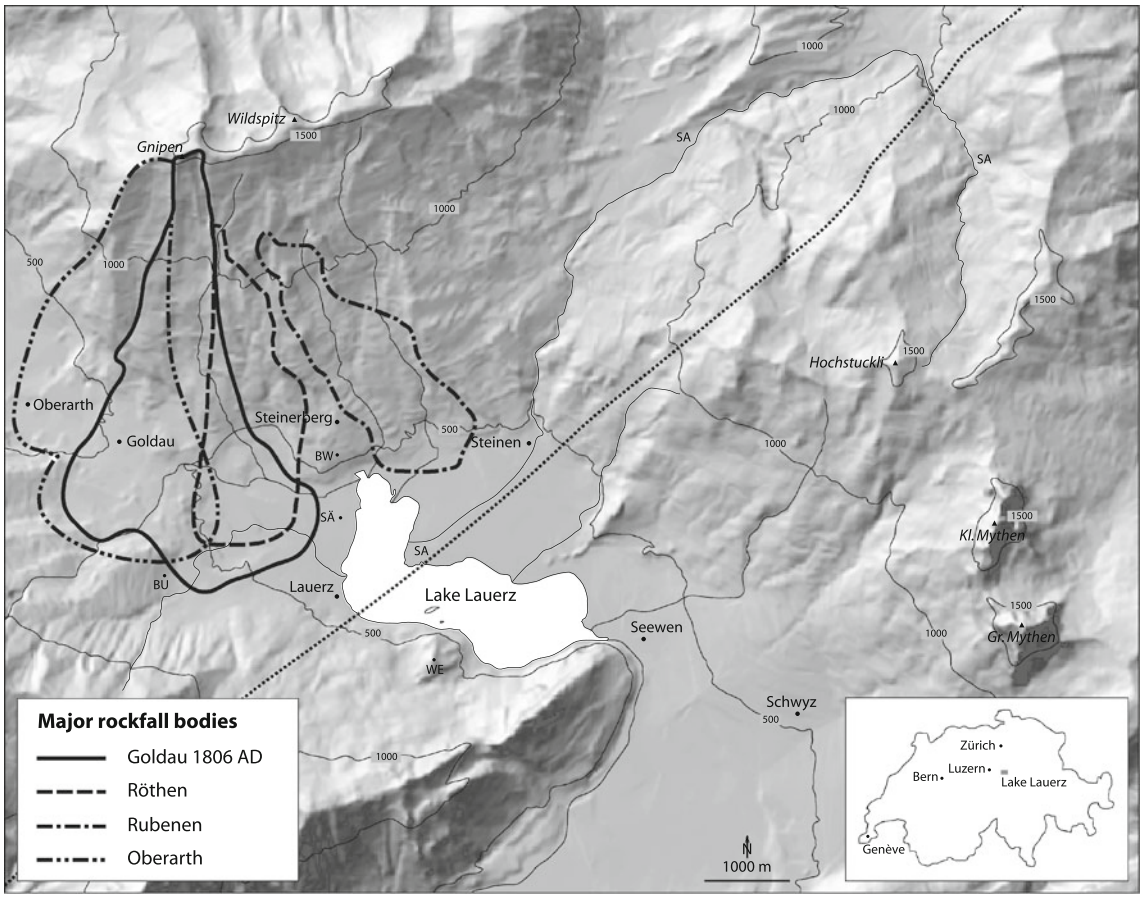

Fig. 1 Lake Lauerz and its catchment. The *dotted line* indicates the North-Alpine nappe front, which broadly separates the Helvetic Nappes in the southeast from the Subalpine Molasse in the northwest. Gnipen and Wildspitz are the two main summits of the Rossberg chain. The limits of four major rockfall bodies are outlined with *bold lines* (after Gasser 2003). Locations referred in the text are indicated with *tokens*: *SA* Steiner Aa, *SÄ* Sägel, *BU* Buosigen, *WE* Weidstein, *BW* Blattiswald. Topographic map and digital elevation model by swisstopo

of the 1806 AD event, the 'Rubenen Bergsturz' and the 'Oberarther Bergsturz', are of prehistoric postglacial age (Gasser 2003). The latter involved an even larger volume of failing rock than the 1806 AD event (Fig. 1) and can thus be regarded as the biggest mass wasting event in the Rossberg rockslide succession (Kopp 1936). However, the present knowledge about the Rossberg landslide history is scarce, since exact datings of the different mass wasting events are lacking. In this study, a new approach to reconstruct this history is presented.

Lake sediments provide some of the most precise natural archives that might record past environmental changes (e.g. Last 2001; Gilli et al. 2005; Anselmetti et al. 2006) as well as past extreme events such as floods (e.g. Brown et al. 2000; Noren et al. 2002; Gilli et al. 2003), earthquakes (e.g. Schnellmann et al. 2002; Becker et al. 2005; Strasser et al. 2006) or subaerial and subaqueous mass movements (Sletten et al. 2003; Schneider et al. 2004; Schnellmann et al. 2005). Such exceptional events often create a characteristic sedimentological fingerprint within the lake deposits, which can be analyzed with standard limnogeological methods. Moreover, different dating techniques provide an excellent time control and allow a highly-resolved reconstruction of these past events. A landslide-generated impulse wave, as triggered by the 1806 AD sliding event or by any of the large prehistoric slides, is likely to have left a characteristic sedimentary pattern in the lacustrine deposits, even in the slide-distant areas of Lake Lauerz. The main goals of the present study are (1) recognition of the sedimentological fingerprint created by the 1806 AD sliding event, (2) scanning the sedimentary archive for similar patterns that were created by comparable preceding events and (3) dating of detected events within the sedimentary record in order to reconstruct the mass movement history of Lake Lauerz. Further goals include (4) the reconstruction of flood event history based on recovered and dated flood layers and (5) reconstruction of the infilling rates to predict the future evolution in morphobathymetry of Lake Lauerz, as concerns arose among local authorities and lake-side communities that an already shallow bay could soon be separated from the rest of the lake due to high infill rates.

Study site

Lake Lauerz is a perialpine lake at an altitude of 447 m.a.s.l. situated in the Canton of Schwyz, Central Switzerland. Erratic blocks, which were transported by the Reuss-Glacier, can be found in several locations around the lake (e.g. Blattiswald, Weidstein, Buosigen; see Fig. 1 for geographical locations) and confirm the glacial overprint of the lake's surroundings (Gasser 2003). Two main theories concerning the lake's origin and evolution prevail: Gasser (2003) suggests a mainly glacial origin of the lake whereas Kopp (1960) and Thuro et al. (2006) contend the lake to be the product of the postglacial, prehistoric Oberarther Bergsturz, which reportedly was able to dam a former river that was discharging into Lake Zug in the west. Lake Lauerz has a surface area of 3 km^2 and occupies a NW-SE trending trough, with two main basins that are divided by a ridge (Fig. 2a) formed by nummulitic limestone outcropping on two islands, along which methane exhalation in the order of 1,000 m^3 day^{-1} occurs (Büchi and Amberg 1983). This subaquatic ridge marks the North-Alpine nappe front, a major, SW-NE striking tectonic overthrust, which broadly divides the Helvetic Nappes in the SE from the Subalpine Molasse in the NE (Fig. 1).

The lake's western basin reaches a depth of 10 m whereas the maximum depth of 13 m is located in the eastern basin (Fig. 2a). Besides the two main basins, Lake Lauerz is composed of a northwestern bay, where the river Steiner Aa nowadays enters the lake through a fast growing delta. 28.5 km^2 of the total catchment area of 69 km^2 account for this main tributary (Lambert and Pfeiffer 1990). The rest of the tributaries are of minor importance in terms of sediment supply, since they are all fed by catchments with a surface area of less than 8 km^2 each. A study, which was based on diatom assemblages, focused on the trophic state of Lake Lauerz and revealed a considerable human impact on the lake's ecology expressed in a shift from rather mesotrophic conditions before 1960/1970 to a highly eutrophic state from 1970 to 1980 (AquaPlus 2002, 2006). In the last 20 years, nutrient concentrations decreased again due to water protection measures approaching slowly a trophic state as observed before 1960.

The catchment geology can be roughly subdivided into four members: (1) In the SE of the catchment, marls and limestones (Helvetic borderchain) of Early Cretaceous age occur. Presumably, their contribution to the lacustrine sedimentation in Lake Lauerz is small, due to their narrow extent and the lack of significant streams originating in this area. (2) Clastic deposits consisting of turbiditic calcareous sandstones with graded bedding intercalated by marly shales outcrop around the upper course of the Steiner Aa in the NE of the catchment ('Wägitaler Flysch'). These flysch sediments were deposited in the Penninic realm during the Late Cretaceous. (3) Eocene limestones, which are often iron-bearing and abundant in nummulites ('Einsiedeln Formation') associated with marly sediments ('Stad Mergel') compose the Subalpine 'Randflysch', which transects the lake from SW to NE, forming the above described subaquatic ridge (Hantke 2006). (4) The greatest portion of the lake's catchment corresponds to sediments of the Subalpine Molasse composed of thick conglomerates interstratified with thinner beds of marls and sandstones,

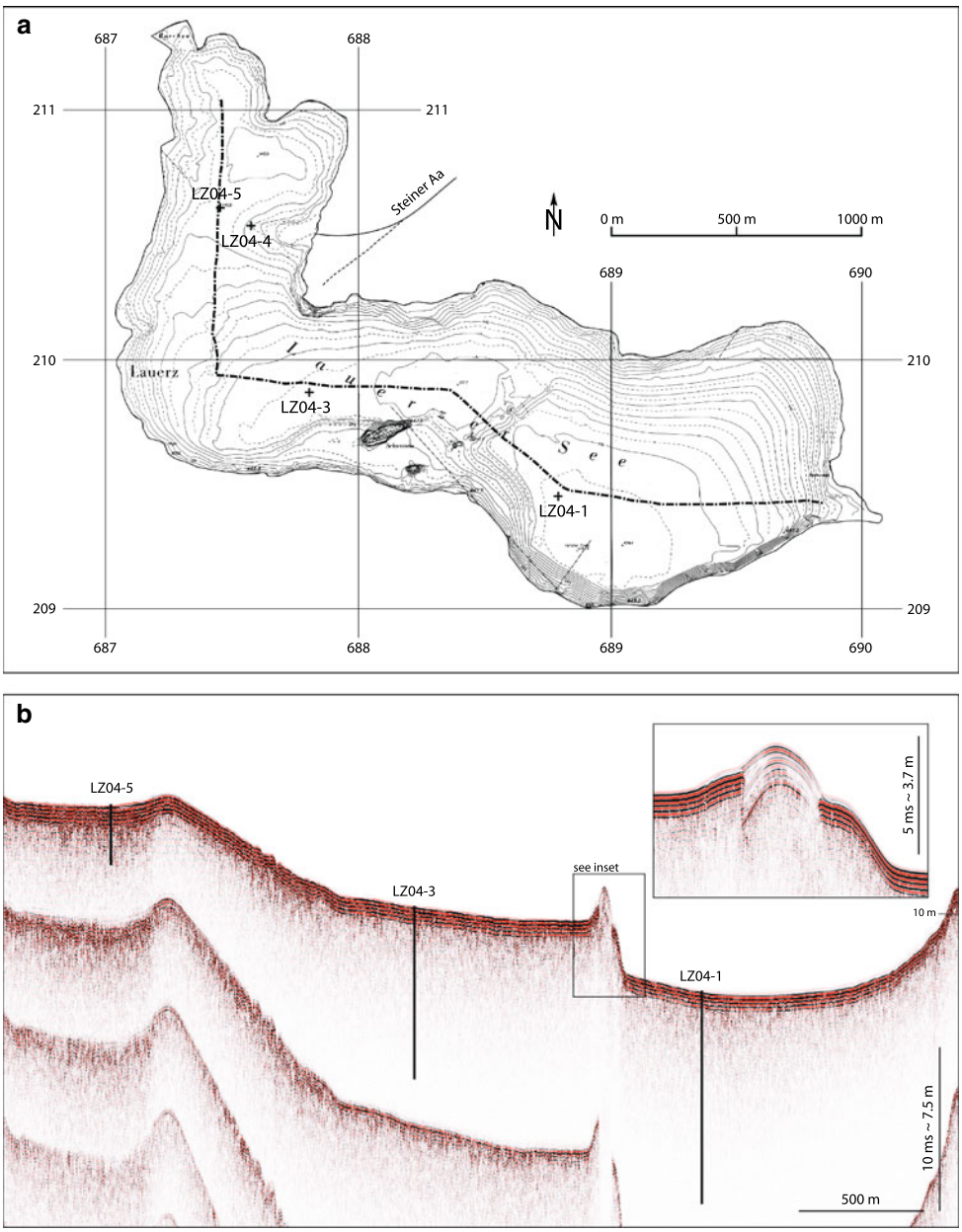

Fig. 2 **a** Bathymetry of Lake Lauerz. Contour interval of *solid lines* is 1 m, 0.5 m steps are additionally indicated by *dashed lines*. Water surface is at 447 m.a.s.l. The course of the modern and ancient Steiner Aa is indicated with *bold solid* and *bold dashed line*, respectively. Coring locations are emphasized with *crosses*. Modified after Lambert and Pfeiffer (1990). **b** *Longitudinal seismic line* (vertically exaggerated) along Lake Lauerz with the water surface at the top margin. Ship track is indicated on the bathymetric map *above*. The division of the lake basin into three subbasins is clearly visible: A shallow northwestern bay, the western basin and the eastern basin comprising the lake's deepest area (13 m water depth). Retrieved sediment cores are projected onto the seismic line. The three to four reflections following immediately after the first lake floor reflection are caused by the ringing of the transducers and are part of the emitted source signal. Note also the strong multiples indicating an almost complete reflection of the seismic energy at the lake floor. *Inset* shows a detailed view of the seismic signal in the area of the subaquatic ridge, which is the only spot in the lake basin where the acoustic signal penetrates the subsurface

which conveys the typical banded aspect to mountains such as Rossberg and Rigi, north and south of the lake respectively (Trümpy 1980). This unit was deposited during Upper Oligocene/Lower Miocene and is generally dipping towards S with angles between 15° and 30° (Thuro et al. 2006).

Especially the shallow northwestern bay of Lake Lauerz is subject to significant aggradational processes, which are mainly caused by the constant sediment supply provided by the Steiner Aa. Gravel extraction in the order of 1,000 m^3 $year^{-1}$ in the lower course of the Steiner Aa is performed since a few decades in order to reduce the supply of coarse sediment and subsequently, the rapid infill of the lake (Lambert and Pfeiffer 1990). On its western end, Lake Lauerz is delimited by the Sägel, an ample swamp of outstanding botanical and zoological interest, which is the remnant of a very shallow former part of the lake (Gasser 2003). This area also was affected by parts of the 1806 AD rock avalanche and, possibly, by preceding mass wasting events that diminished the lake's original size vastly. Numerous conglomerate boulders that can be found in the area witness these processes.

Methods

A single-channel reflection seismic survey was performed in order to (1) image the geometries of the lacustrine

sediments, (2) detect possible event layers due to distinct seismic facies, (3) determine appropriate coring locations for the retrieval of both, short and long cores, and (4) generate a bathymetric map. The seismic equipment consisted of a 3.5 kHz Geoacoustic Pinger source/receiver. The Pinger was mounted on an inflatable cataraft that was pushed in front of a Zodiac raft. Raw data were recorded in SEG-Y format and subsequently processed, applying a time variant bandpass filter.

In 2004, two short gravity cores and four long piston cores were retrieved from four different locations. Coring sites are indicated in Fig. 2a and b. The recovery of the short cores was performed using an ETH short coring device consisting of a weight-armed top part on which a PVC-liner is attached. Maximum length of the short cores was 1 m. The long cores were retrieved using an Uwitec piston-coring device mounted on a platform with inflatable floats. The maximum coring depth of 9.77 m was achieved in the deepest part of the lake in the eastern basin. Physical core logging including p wave velocity, gamma-ray attenuation bulk density and magnetic susceptibility was performed on the non-splitted core sections in 5 mm-intervals using a GEOTEK multi-sensor core logger. Further core preparation included opening, photographing and visual description of the cores. As the long cores were retrieved in 3 m-sections with overlaps of 50 cm, a composite section for every coring location was established based on visual correlation of the split cores. For the uppermost section this composite section consisted also of the short cores taken at the same location. In the following sections and figures, depth values always refer to this composite depth scale. Bended strata, as visible in some core photos within this manuscript, are the product of the coring method applied and must thus be regarded as artifacts. Furthermore, high gas contents within the sediments have led to significant coring disturbances, making the definition of the above mentioned composite section particularly challenging. No regular sampling interval but rather targeted sampling within visually outstanding sedimentary layers was performed. Grain size was analyzed using a laser-optical Malvern Mastersizer 2000 device. Furthermore, a UIC Inc.™ coulometer was used for the determination of the total organic carbon (TOC) and total inorganic carbon (TIC; a measure for carbonate content).

A total of five samples were extracted from the two basinal cores LZ04-1 and LZ04-3 and submitted to the radiocarbon lab at ETH Zürich for accelerator mass spectrometer (AMS) ^{14}C dating. All samples consisted of terrestrial plant macrofossils (leave remains and in the case of the lowermost/oldest dating a wood fragment) that were washed out of the sediment with distilled water using a fine sieve. Dates were calibrated using CALIB v 5.0.1 (Stuiver and Reimer 1993; Stuiver et al. 1998) and are reported in calendar years (AD).

Lacustrine lithologic succession of Lake Lauerz

Reflection seismic profiles

All seismic lines of Lake Lauerz show little to no penetration of the seismic signal into the lacustrine sediments and do therefore not provide valuable subsurface information (Fig. 2b). Only the area of the subaquatic ridge separating the two deep basins shows few seismic subsurface reflections (Fig. 2b, inset). Poor seismic penetration is not unusual in alpine and perialpine lakes and has been reported previously by several authors (e.g. Giovanoli et al. 1984; Niessen 1987; Leemann 1993; Gilli et al. 2003). It is most likely originating from high gas contents within the sediment, either due to decomposition of organic matter or by the observed exhalation of fossil methane, which is dispersed through the sedimentary column. Rising gas bubbles during coring operations confirmed the assumption of gas rich sediments in the subsurface of Lake Lauerz.

Delta cores

Two long piston cores were retrieved in front of the prograding delta of the Steiner Aa in order to recover the Rossberg-proximal landslide signature and to quantify the sediment budget provided by this major tributary and subsequently predict the future infill of the apparently shallowing and shoaling northwestern bay to the north of the delta. Core LZ04-4 (hereafter named core 4) was retrieved on the delta itself in 2.5 m water depth whereas core LZ04-5 (hereafter named core 5) was extracted in a more delta-distal area in a water depth of 3.9 m on a smooth topographic saddle, which nowadays divides the mentioned northwestern bay from the rest of the lake (see Fig. 2a for core positions). We identified three Lithologic/Lithostratigraphic Units D1–D3 ('D' for delta), which can be correlated among both cores based on the visual description of the sediments as well as their petrophysical properties (Fig. 3).

Unit D1 (0–255 cm in core 4; 0–87 cm in core 5) consists of a dark yellowish brown, faintly-laminated clastic silt intercalated by layers of coarser sediment (fine to medium sand and fine sand in core 4 and 5, respectively), which partially contain coarse organic debris (terrestrial plant macrofossils at mm-scale). These intercalated layers can be as thick as 15 cm in core 4 and up to 10 cm in core 5. In core 4, the silty background sediment shows bulk densities of 1.7 g cm^{-3}, whereas the coarse layers reveal

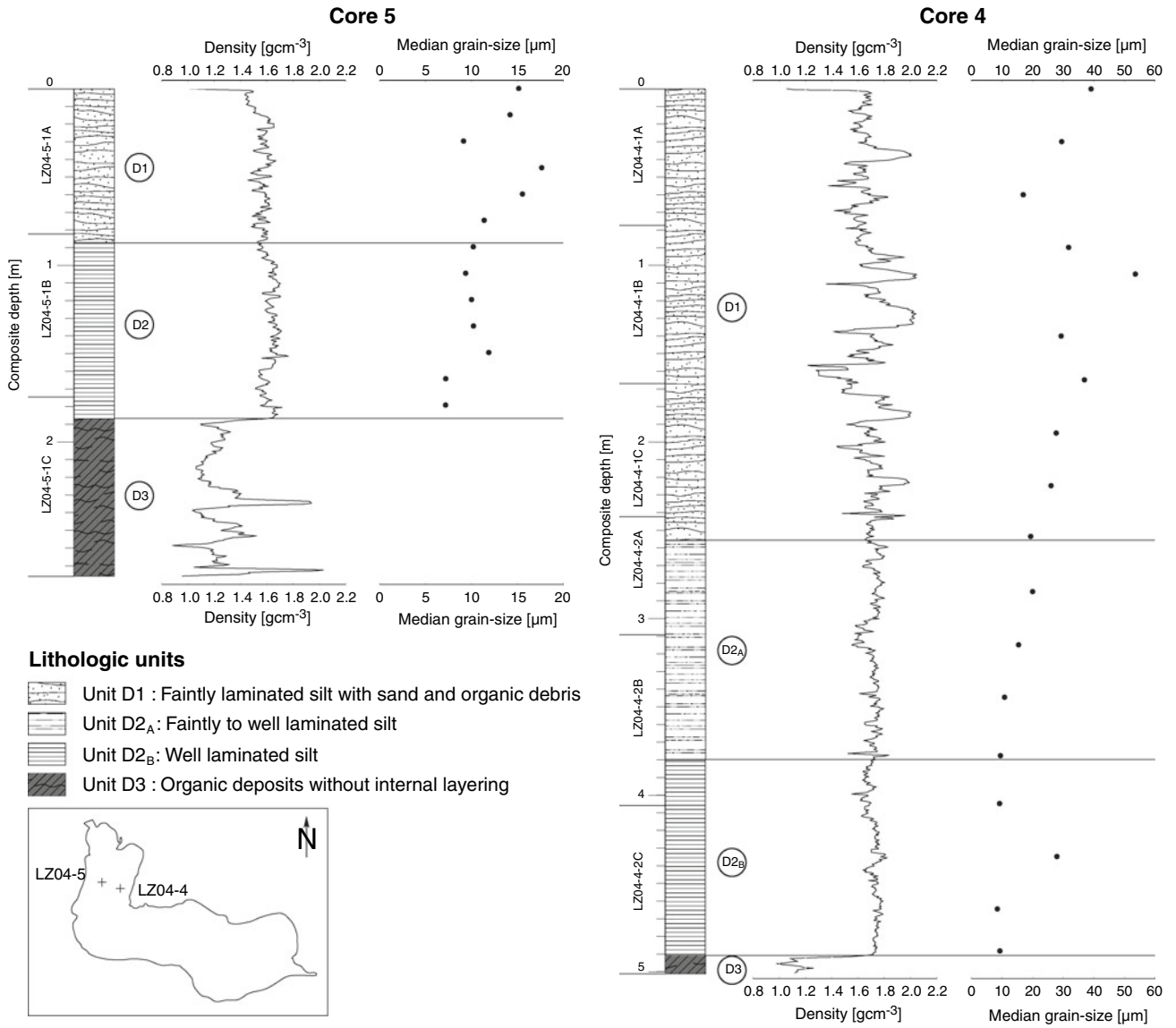

Fig. 3 Lithologic sections of delta cores 5 (*left*) and 4 (*right*) with density as well as measured grain size data. Lithologic Units are emphasized with *encircled letters*. Codes of the individual core sections are indicated to the *left* of the sections

density values of 1.4–1.5 g cm^{-3} when associated with organic debris and 1.9–2.0 g cm^{-3} without organic debris, respectively. In contrast, bulk density of Unit D1 is rather constant in core 5, reaching an approximate mean value of 1.55 g cm^{-3}. Due to the occurrence of the intercalated coarse-grained layers, median grain-size is varying strongly between 17 and 54 µm in core 4 and in the range of 9–18 µm in core 5.

Underlying Lithologic Unit D2 can be split up into two subunits in core 4: Unit $D2_A$ (255–380 cm) consists of pale to dark yellowish brown, faintly to well-laminated clastic silt intercalated by coarser layers (fine sand) of few cm thickness, which in contrast to the sand layers of Unit D1 do not show significant density peaks. Layers containing organic debris comparable to those of Unit D1 are scarce and only a few cm-thick. The whole unit shows a rather uniform bulk density of 1.7 g cm^{-3}. Median grain-size is continuously increasing upwards from 9 to 20 µm; Unit $D2_B$ (380–491.5 cm) is composed of pale yellowish brown, well-laminated clastic silt. No coarse organic debris is present and intercalated layers of fine sand are scarce with thicknesses below 1 cm. The bulk-density curve for this unit shows a very uniform pattern with a mean value of 1.75 g cm^{-3}. Similarly, median grain-size is quite constant with values around 9 µm. In core 5, Unit D2 (87–187 cm) contains pale to dark yellowish brown, well-laminated clastic silt punctuated by up to 3 cm-thick, normally-graded layers with bases of fine sand and elevated content of fine organic detritus. These layers are easily recognizable also due to their rather grayish color. No coarse organic

debris as described for Unit D1 is found within Unit D2. Density is quite constant showing a mean value of 1.65 g cm^{-3}. Within this unit, median grain-size is increasing upwards from 7 to 10 µm in core 5.

In both cores, Unit D2 is delimited at its base by a sharp transition from the visually outstanding Unit D3 (below 491.5 cm in core 4; below 187 cm in core 5) consisting of dusky brown, organic 'peaty' deposits with no persistent internal layering (Fig. 4a). These deposits are interfingered on several spots by brighter-colored, calcite-bearing lacustrine sediments (Fig. 4b). The transition from Unit D2 to Unit D3 is marked by a major downcore drop in the bulk density to 1.1–1.2 g cm^{-3} (Fig. 3). In core 5, positive density anomalies of up to 2 g cm^{-3} result from several rock pebbles of maximum 4 cm-diameter, which can be found throughout the whole unit below 230 cm subsurface depth. These pebbles, which are mostly well-rounded and partially coated with remnants of an orange to reddish-colored sandy matrix, can clearly be attributed to the conglomeratic rocks of the Subalpine Molasse outcropping in the Rossberg area to the north of the lake. In both cores, the base of Unit D3 was not reached through coring.

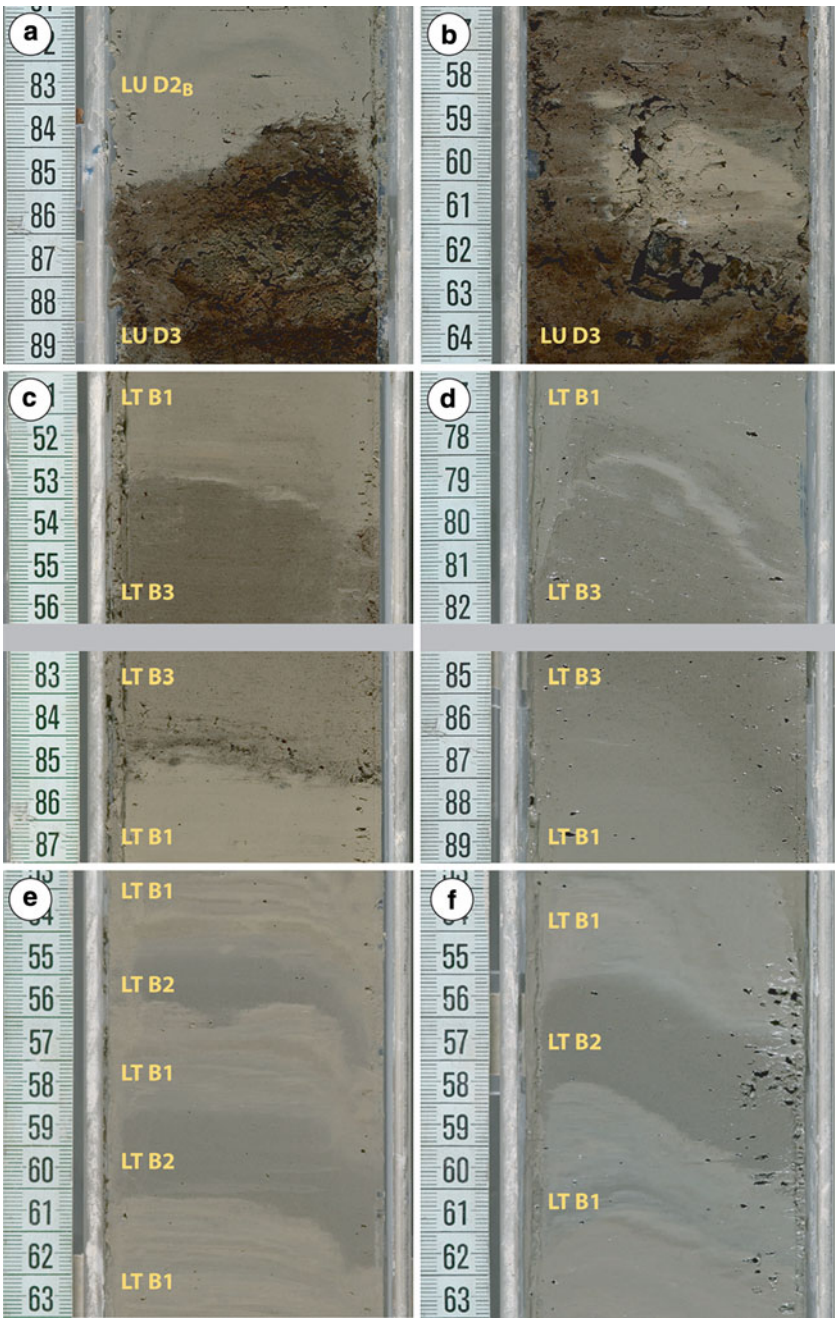

Fig. 4 Photographs of sediment cores. Coring positions are indicated in Fig. 2. The scale that is given on the *left* edge of the pictures does not correspond to the composite depth of the cores. Bending of layers results from coring disturbance. Core photographs from delta cores 4 (**a**) and 5 (**b**). (**a**) Sharp transition from the organic-rich deposits of Lithologic Unit (LU) D3 (*below*) to the lacustrine sediment of LU $D2_B$ (*above*). (**b**) Patch of carbonate bearing lacustrine sediment, which is embedded in the organic-rich deposits of LU D3. Core photographs from basinal cores 3 (**c**) and 1 (**d**) showing the Lithotype (*LT*) B3-layers deposited by the 1806 AD mass wasting event. Note that the layers are not shown in full extent. (**c**) The top of the 1806 AD LT B3-layer in landslide-proximal core 3 is characterized by a bright, whitish cap. The transition from the underlying LT B1 sediment to the 1806 AD LT B3-layer is also clearly visible. (**d**) The top of the 1806 AD LT B3-layer in landslide-distal core 1 is characterized by a similar bright, whitish cap as within the same layer in core 3. Transition from underlying background sediment (LT B1) to 1806 AD LT B3-layer is rather faint. Core photographs from basinal cores 3 (**e**) and 1 (**f**) showing the background sedimentation (LT B1), which is irregularly intercalated by LT B2 layers, recognizable by their rather dark gray color

Basinal cores

In order to track the sedimentological fingerprint left by the 1806 AD rock avalanche, by the possibly preceding events and by extreme floods, we retrieved two long piston cores in the two main basins of Lake Lauerz. Coring was focused on the almost flat basin plains of the respective basin, where the sedimentary succession is most continuous. Core LZ04-1 was retrieved in the eastern basin where the lake reaches its maximum water depth of 13 m, whereas core LZ04-3 was taken in the western basin in an approximate water depth of 9 m. The total lengths of the composite section are 977 and 794 cm in core LZ04-1 and LZ04-3, respectively (hereafter named cores 1 and 3, respectively). Three different lithotypes B1–B3 ('B' for basin) were described (Fig. 4c–f), which have been recognized in both basinal cores (Fig. 5). Unlike D1–3, these lithotypes B1–3 are not stratigraphic units. They are subsequently characterized upon their sedimentological, petrophysical and geochemical properties: The lacustrine succession in both basinal cores consists mainly of Lithotype B1, which forms the background sediment. Within these deposits, layers of Lithotypes B2 and B3 are irregularly intercalated. Lithotype B1 deposits comprise gray to brown mud partially exhibiting a faintly to well-developed lamination. Macrofossils (mostly terrestrial plant remains) can be found in this lithotype throughout the whole cores. Coulometric determination of carbon content within Lithotype B1 deposits revealed median values in carbonate content of 13.9 and 20.3 wt% in core 1 and 3, respectively. Median values of TOC amount to 1.32 and 1.01 wt% in core 1 and 3, respectively. These values document a strong gradient in the amount of carbonate and the portion of organic carbon that is deposited and preserved with respect to the distance to the main sedimentary source (Steiner Aa). Notably, the carbonate portion decreases with increasing distance to the river estuary whereas the opposite trend is valid for the occurrence of organic carbon.

Layers of Lithotype B2 can easily be distinguished from the background sedimentation (B1) by their rather dark gray color (Fig. 4e, f). Additionally, they are often blackish mottled due to the occurrence of fine plant macrofossils. These macroremains are clearly of terrestrial origin (wood and leaves), pointing towards a terrestrial, clastic sediment input, as described in other lakes (Brown et al. 2000). Lithotype B2 layers can be as thick as 7 cm in core 1 and 11 cm in core 3 and are commonly associated with positive density peaks, reaching values of up to 1.7–1.8 g cm^{-3}. Grainsize analysis reveals an often normally graded pattern within layers of Lithotype B2. The carbon portion within Lithotype B2 is almost equally distributed between TOC (median values of 1.60 and 1.92 wt% in core 1 and core 3, respectively) and TIC (median values of 1.47 and 1.86 wt% in core 1 and core 3, respectively). The TIC corresponding carbonate values are 12.2 and 15.5 wt% in core 1 and core 3, respectively. In contrast to the pattern described for the Lithotype B1, both, carbonate and TOC values are increasing with increasing distance to the main sedimentary source. In average, Lithotype B2 layers occur 5.5- and 8.5-times per meter in core 1 and 3, respectively. Previous work has demonstrated that such terrigenous layers are deposited by exceptional runoff events when rainfall of great intensity and/or duration affects mountainous lake drainage basins (Eden and Page 1998; Brown et al. 2000; Chapron et al. 2002; Noren et al. 2002; Gilli et al. 2003). Therefore, we interpret those frequently occurring strata as flood layers, which were deposited during episodically strong rainfall events in the catchment of Lake Lauerz. Such exceptional runoff events have led to a temporarily increased transport capacity of the tributaries, mainly the Steiner Aa, inducing the formation of sediment-laden density currents, bringing a large amount of clastic sediment into the center of the lake basin. Comparable flood horizons have been used to reconstruct the chronology and periodicity of major storms in a lake's catchment (e.g. Eden and Page 1998; Brown et al. 2000; Noren et al. 2002; Gilli et al. 2003).

Lithotype B3 comprises layers of light to dark brownish sediments, which commonly show negative density peaks and often exhibit a high abundance of coarse organic macroremains. They are normally graded, can be as thick as 20 and 32 cm (core 1 and 3, respectively), and do represent the most prominent layers intercalating the background sediment (Lithotype B1). Due to the high occurrence of organic material, TOC contents (median values of 2.42 and 3.00 wt% in core 1 and 3, respectively) are generally higher than corresponding TIC/carbonate contents (median values of 1.64 TOC/13.6 wt% $CaCO_3$ and 2.13 TOC/17.7 wt% $CaCO_3$ in core 1 and 3, respectively), what serves, next to the color and density, as main proxy for distinguishing lithotype B3 from B2. Lithotype B3-strata are interpreted as layers, which contain the sedimentological fingerprint left by major mass wasting events (see below).

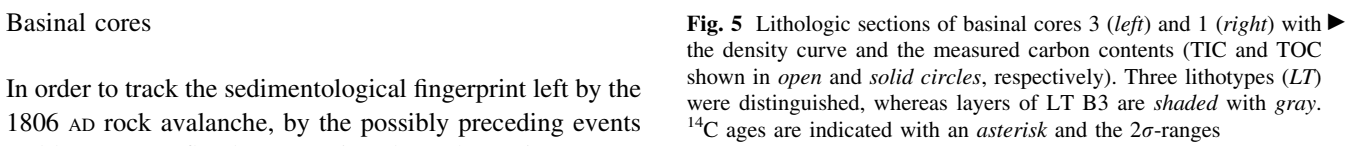

Fig. 5 Lithologic sections of basinal cores 3 (*left*) and 1 (*right*) with the density curve and the measured carbon contents (TIC and TOC shown in *open* and *solid circles*, respectively). Three lithotypes (*LT*) were distinguished, whereas layers of LT B3 are *shaded* with *gray*. ^{14}C ages are indicated with an *asterisk* and the 2σ-ranges

Sedimentological fingerprint of the 1806 AD event

Proximal signature

The most conspicuous feature within both delta cores is the visually outstanding Unit D3, which shows sedimentological

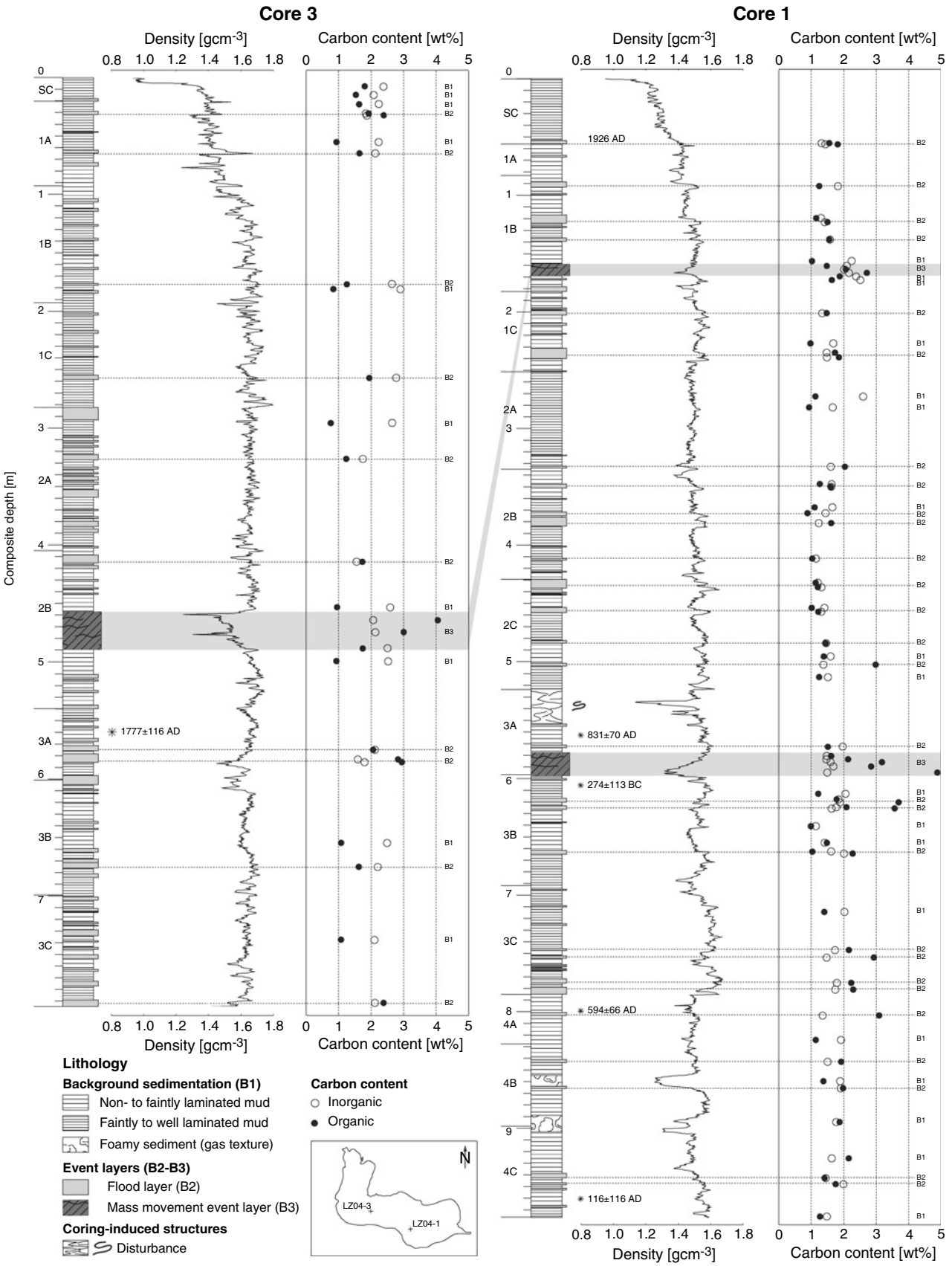
Core 3
Core 1
Density [gcm-3]
Carbon content [wt%]
Composite depth [m]
SC
1A
1
1B
2
1C
3
2A
4
2B
5
3A
6
3B
7
3C
8
4A
4B
9
4C
1777±116 AD
1926 AD
831±70 AD
274±113 BC
594±66 AD
116±116 AD
B1
B2
B3
Lithology
Background sedimentation (B1)
Non- to faintly laminated mud
Faintly to well laminated mud
Foamy sediment (gas texture)
Event layers (B2-B3)
Flood layer (B2)
Mass movement event layer (B3)
Coring-induced structures
Disturbance
Carbon content
Inorganic
Organic
N
LZ04-3
LZ04-1

and petrophysical patterns totally differing from those observed within the overlying Units D2 and D1. The sediments comprised in Unit D3 are mostly of a non-lacustrine source and only few intercalated carbonate-bearing spots of lacustrine sediment can be found. We interpret the sediments of Unit D3 to be initially deposited under subaerial or swampy conditions, as it is supported by the high abundance of well-preserved terrestrial plant macrofossils and tiny plant roots, which interfinger the deposits on several spots. The deformed lake sediment pieces contained within D3 and the lack of physical mechanism to explain a lake level lowering make us interpret these D3-deposits as lakeward displaced swamp material. On its top, they are sharply overlain by lacustrine delta sediments, which comprise the chronologically subsequent Units D2 and D1. We suggest that Unit D3 was transported into the lake basin by a gravity spreading-induced mobilization of swamp material, which was provoked by the loading of the accumulating sliding mass on top of mechanically weak swamp deposits during the 1806 AD rock avalanche.

Distal signature

In basinal core 3, we interpret a 32 cm-thick B3-layer in 457–489 cm depth to be the product of the 1806 AD landslide event. The mottled, dark brownish color sharply contrasts the over and underlying background sediment, and its thickness is almost three times as high as the thickness of the second-thickest layer of either lithotype B2 or B3. At its bottom, the layer is separated by a coarse fining-upward base from the background sediment, whereas a bright, whitish cap is marking its top (Fig. 4c). A significant density low with a decreasing upwards pattern and very high TOC values are additional features, which punctuate the exceptional characteristics of this layer. The remarkably high content in TOC of 4 wt% can directly be explained to be the product of the laterally displaced organic swamp deposits, which were mobilized into the water body (see above).

In the landslide-distal of the two basinal cores (core 1), a similar, albeit thinner layer of lithotype B3, can be found at 158–168 cm subsurface depth (Fig. 4d), which we interpret to be the product of the 1806 AD landslide event. This preliminary assumption is supported by sedimentation rates revealed in a previous study, which dated the topmost sediment recovered by a core in the immediate proximity of coring location 1 using a ^{137}Cs-profile (AquaPlus 2002). An approximate bulk sedimentation rate of 1 cm year^{-1} resulted for the last 18 years, a value which is highly similar to the bulk sedimentation rate of 0.8 cm year^{-1} for the last 200 years as inferred from the assumption made here. However, the slight discrepancy between the two values is most likely caused by stronger compaction in the deeper sediments. As its counterpart in the landslide-proximal basinal core, the layer shows elevated contents in organic matter, decreased density values and a bright, whitish cap on its top (Fig. 4d). The base of the layer appears to be smeared since a rather gradual transition from the underlying background sediment is visible (Fig. 4d). The observed differences between the proximal and the distal fingerprint at the base of the layer most likely result from a change in the sediment transport capacity, which could be caused by the increasing distance to the sedimentary source (mobilized swamp and eroded lake sediment) and/or by the subaqueous ridge, which divides the two basins and thus acts as a topographic barrier with significant influence in the flow conditions during major mass wasting events.

Age model and sedimentation rates

The chronology of basinal core 1 is based on the sedimentological recognition of the 1806 AD event-layer, supported by ^{137}Cs dating of the topmost sediment performed by a previous study (AquaPlus 2002), and a total of four AMS ^{14}C ages. Radiocarbon ages were calibrated using CALIB v 5.0.1 (Stuiver and Reimer 1993; Reimer et al. 2004) and are reported in Table 1. Linear interpolation among these well-constrained datings have led to a consistent age model for core 1 (Fig. 6). The age model was defined as straight segments through the center of the

Table 1 Radiocarbon dates for cores LZ04-1 and LZ04-3, Lake Lauerz, Switzerland

Core	Section	Section depth (cm)	Comp. depth (cm)	Lab. number	Material	^{14}C age (years BP)	δ13 C (‰)	2σ calib. mean (AD)	1σ calib mean (AD)
LZ04-1	3A	69	562	ETH-32360	Leaf remains	1195 ± 45	−24.3 ± 1.2	831 ± 70	832 ± 58
LZ04-1	3B	9	606	ETH-32361	Leaf remains	2195 ± 45	−28.0 ± 1.2	274 ± 113 BC	317 ± 40 BC
LZ04-1	4A	51	800	ETH-32472	Leaf remains	1470 ± 55	−26.9 ± 1.2	594 ± 66	597 ± 45
LZ04-1	4C	62	960	ETH-32362	Wood fragment	1910 ± 50	−29.1 ± 1.2	116 ± 116	80 ± 57
LZ04-3	3A	54	560	ETH-32471	Leaf remains	155 ± 55	−27.6 ± 1.2	1,777 ± 116	–

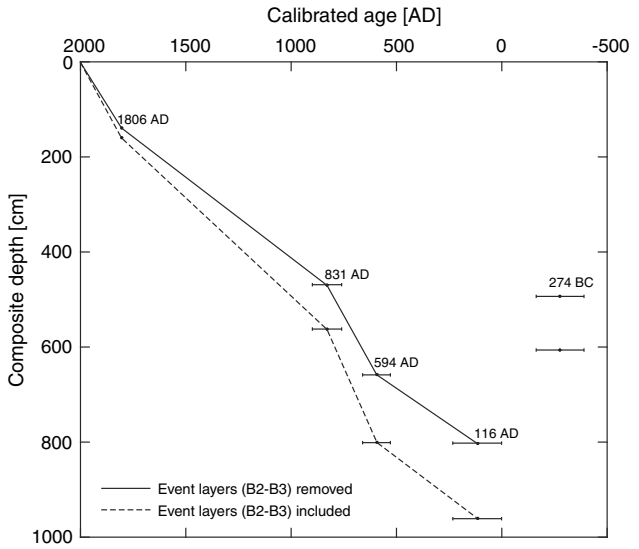

Fig. 6 Age models of core 1 based on sedimentological evidences and 4 AMS ^{14}C datings. *Dots* represent mean values of 1σ-ranges whereas error *bars* indicate 2σ-ranges. All dates were calibrated with CALIB v 5.0.1. The age model considering bulk sedimentation-rates (including event layers LT B2 and B3) is indicated by *dashed lines*, whereas the age model based on background sedimentation-rates (event layers LT B2 and B3 removed) is drawn with *solid lines*. For the purpose of establishing a concise event chronology, the age model on the basis of background sedimentation was used in this study

1-sigma range of the radiocarbon dates and the 1806 AD event marker. The two-sigma bars in Fig. 6 visualize the uncertainty of the age model. However, sample ETH-32361 (2,195 ± 45 ^{14}C years BP), which was taken close to sample ETH-32360 (1,195 ± 45 ^{14}C years BP) is apparently not fitting into the overall downcore trend indicated by the other datings. This age is interpreted to mark an older reworked component and was therefore not included into the core chronology.

Because event layers as recognized in lithotypes B2 and B3 sediments do not represent significant time within the chronology, but do represent a significant thickness (Eden and Page 1998), two different age models were established. In a first step, bulk sedimentation rates were calculated, whereas in a second step background sedimentation rates were deduced after removing the recognized event layers. The latter procedure allows for a more accurate dating of individual event layers occurring between the fixed ages in core 1 assuming constant sedimentation rates between successive age constrain points. Bulk sedimentation rates within the last 2,000 years varied considerably between 0.33 and 1.00 cm year^{-1} (Fig. 6), whereas this variation is slightly less pronounced when considering only background sedimentation rates, which vary between 0.30 and 0.79 cm year^{-1}.

Significantly higher sedimentation rates within core 3 are the product of a more direct influence of the Steiner Aa sediment supply into the western basin. In this core, the chronology is solely based on the sedimentary recognition of the 1806 AD event layer (Lithotype B3). This layer is found in a subsurface depth of 457 cm resulting in a bulk sedimentation rate of 2.31 cm year^{-1} and a corresponding background sedimentation rate of 1.83 cm year^{-1} for the post-1806 AD time. An additional radiocarbon sample (ETH-32471) in a composite depth of 559.5 cm revealed a 2σ-range of 1,777 ± 116 AD, confirming the absence of a major erosional discordance at the bottom of the 1806 AD event layer. However, due to its rather high error compared with the absolute age of the sample, the dating cannot be used for a further refinement of the chronology within core 3.

Discussion

Impulse wave generation

Our data indicate that, unlike the frequently made assumption (e.g. Heim 1932), the immediate impact of the rock mass into the water body was *not* the major trigger for the reported catastrophic impulse wave. Rather, this wave was caused by the sudden, gravity spreading-induced lateral displacement of a significant amount of swamp deposits into the lake basin (Fig. 7a, b). Gravity spreading effects, as proposed in this study, were previously described for the subaqueous realm, where accumulating mass-movement deposits induced the formation of basinal fold-and-thrust belt structures due to the successive loading of the slope-adjacent basin-plain sediment (Schnellmann et al. 2005). The fact that west of Lake Lauerz major amounts of large boulders can only be found within a considerable distance away from the pre-1806 AD shoreline as reconstructed by Gasser (2003) additionally supports the concept of wave-triggering by rapid swamp mobilization. Moreover, sixteen years-old eyewitness David Alois Schmid, who observed the rock avalanche from his hometown Schwyz located 2 km east of the lake, clearly illustrated a mechanism, which is quite similar to the one described here in his famous painting 'Der Bergsturz von Goldau 1806', which nowadays represents the probably best known illustration of the devastating catastrophe (Fig. 8). Therein, the falling rock mass is accumulating far beyond the western shoreline on a swampy plain. Vegetation-covered slices of the substrate of this plain are ejected towards the lake in ridges reaching heights of small buildings and thereby acting as potential trigger for disastrous impulse waves within the water body (see detail, Fig. 8). Another congruent description of this mechanism is found in Zay (1807), who described the process he witnessed as follows:

Durch eigene errungene Kraft setzte diese besondere Lauwine ihren Blitzeslauf fort; und was noch auffallender

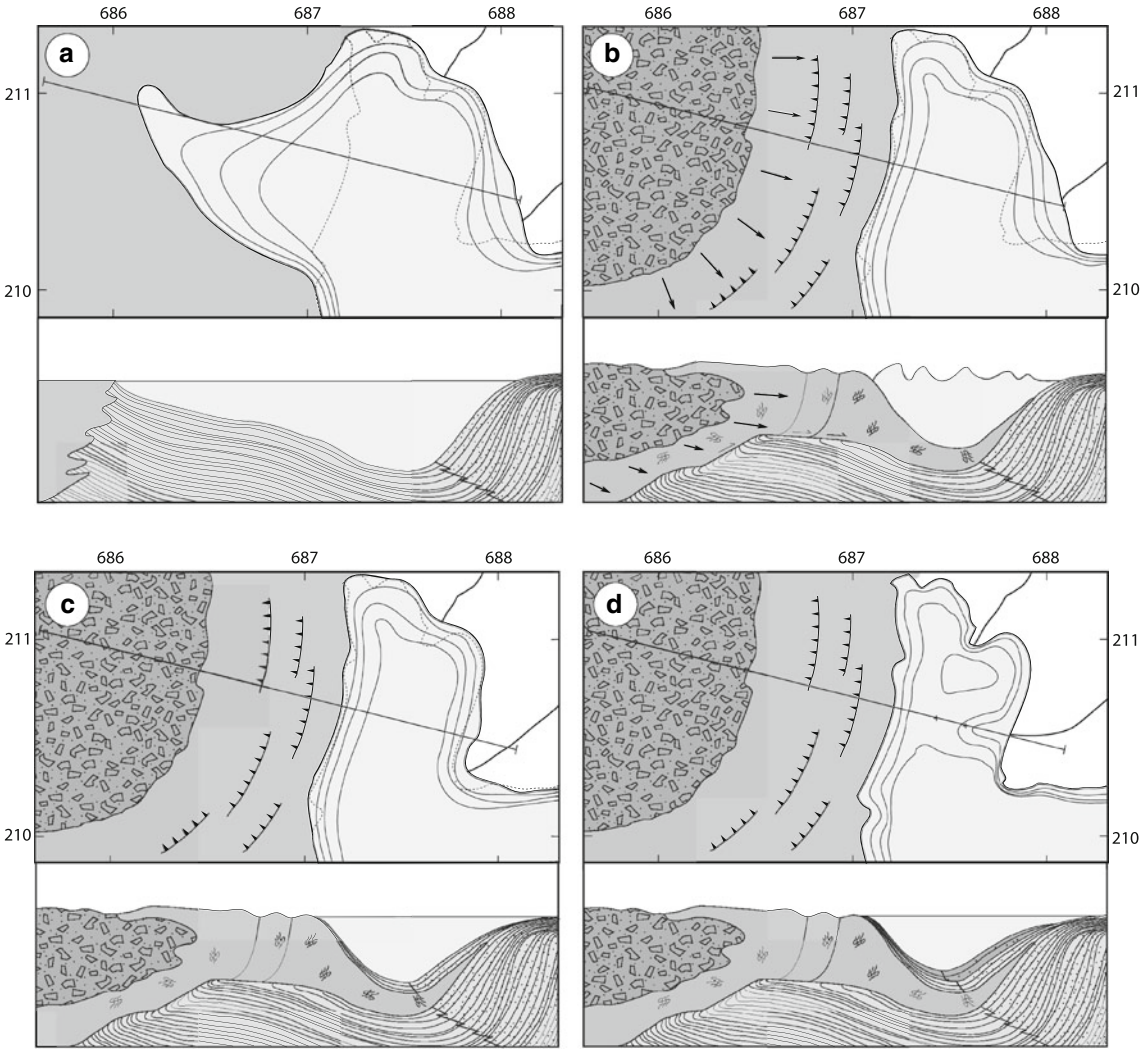

Fig. 7 Schematic sedimentological model proposed for the evolution of the northwestern part of Lake Lauerz within the last 200 years. Note the approximate location of the profiles, furthermore the coring positions of the delta cores are indicated on map *d*. Modern shoreline is indicated on all maps with a *dashed line*. Bathymetrical contours are hypothetical. **a** Pre-1806 AD stage: the shoreline of Lake Lauerz is characterized by a very shallow arm extending into the swamps of Sägel in the west. The river mouth of the Steiner Aa is prograding at 3 m year^{-1} in a southwestern direction. **b** 1806 AD rock avalanche: the accumulation of rockslide debris (*dark gray* with blocky signature) on the mechanically weak swamp deposits (*medium gray*) leads to a gravity spreading-induced mobilization of swamp material and eroded lake sediment into the lake basin and reduces the lake's superficial area by roughly 1/7 of its original size. As a secondary effect, the process triggers the formation of impulse waves of 15 m amplitude. The indicated formation of fold-and-thrust belt structures is hypothetical. However, similar processes were described for the subaqueous realm by Schnellmann et al. (2005). **c** Pre-1934 AD stage: delta sediment (LU D2; *light gray*) is deposited on top of the mobilized swamp (LU D3; *medium gray*). The Steiner Aa is constantly prograding in a southwestern direction. **d** 1934–2006 AD: during a major flood in 1934 AD, the estuary of the Steiner Aa is relocated westwards, corresponding to the sharp transition from LU D2 (*light gray*) to LU D1 (*dark gray*). This event marks the onset of a new progradation direction of the delta, which is associated with the ongoing separation of the shallow northwestern bay from the rest of the lake

war, so borst das Erdreich des Sägels und des dortigen Geländes mit einer ausserordentlichen Bereitwilligkeit in die Höhe, bäumte sich wie flüssige Wasserfluth in Wellen auf, und eilte wogenartig der nachjagenden Lauwinenmasse voran. Sehr merkwürdig muss gewiss jedem Nachdenkenden dies wahrhaft beobachtete Ereignis seyn, und sehr schwer ist es zu begreifen, wie diese Fluthung des Erdreichs sich ergeben, und die ganze Erdenrinde des Sägels und umliegenden Geländes so mit Einmal in die Höhe geworfen, und fluthend habe gemacht werden können.

(Rough translation by the authors: Even more conspicuous was the fact that the soil in the Sägel and surroundings was bursting upwards with exceptional readiness, roaring up in waves like a water surge, and running ahead of the moving rock avalanche mass.)

Fig. 8 Historic painting of the 1806 AD catastrophe drawn by 16 years old eyewitness David Alois Schmid, who observed the rock avalanche from his hometown Schwyz. The entire original painting is shown on the *left* side; with close up of the swampy western shore (Sägel area) on *right* side. Schmid clearly illustrates that upon the impact of the rock masses the substrate of the swampy deposits were laterally ejected towards the lake in vegetated slices reaching heights of small houses. This process subsequently triggered the devastating water waves on Lake Lauerz

Our interpretation implies that the Lake Lauerz impulse wave was not the result of a simple landslide-induced wave generation. Landslide–water body interactions are commonly grouped into three categories including (1) subaerial landslide impacts, (2) partially submerged landslides, and (3) subaqueous or submarine landslides (Fritz 2002). However, none of these categories are applicable to the observed rockslide–water interaction of the 1806 event. The data presented here points towards a conversion from an originally subaerial landslide into a partially submerged landslide–water body interaction as ultimate trigger of the reported impulse waves (Fig. 7a, b) and thus contradicts the prevailing theory that parts of the 1806 AD landslide mass were impacting directly into the western part of former Lake Lauerz. This mechanism implies that an impact-wave hazard is not restricted to areas, where rock masses can fall directly into water bodies, but should be considered also in areas where rockfalls may reach water-adjacent valley plains.

Deltaprogradation and evolution of northwestern bay

Lithologic Unit D3 of the delta-proximal areas, tied to the laterally mobilized swamp deposits of the 1806 AD event, represents an outstanding and well-constrained time horizon implying that the consecutively deposited Units D2 and D1 are the product of roughly 200 years of delta sedimentation. The upwards continuously increasing median grainsize within Unit D2 (Fig. 3) suggests that these sediments were deposited under the immediate influence of a prograding (and thus approaching) feeding system, which in this case can be attributed to the delta formed by the Steiner Aa (Fig. 7c). Heavy rainfall events within the past 200 years episodically increased the sediment transport capability of the feeding river leading to the deposition of the intercalated sandy layers. The transition to Unit D1 is marked by a discrete increase in grainsize and thickness of these flood layers, which can only be explained by the sudden shift of the sediment source (river mouth) closer to the depositional area (coring locations). Since the estuary of the Steiner Aa was naturally relocated westwards in September of 1934 during a heavy rainfall event (Lambert and Pfeiffer 1990), the transition from Unit D2 to Unit D1 is attributed unambiguously to this well-documented event (Fig. 7d). Since then, both coring locations became situated immediately on or in front of the newly developing delta, leading to a substantial increase in median grain-size and thickness of intercalated flood layers within Unit D1.

Lambert and Pfeiffer (1990) report delta progradation rates to be 260 m or 3 m year^{-1} in a southwestern direction for the time interval between 1846 AD and 1934 AD, whereas the modern delta is prograding in a western direction. The resulting potential separation of the northwestern bay has led to concerns among various groups of lake users, resulting in different political demands for remedy measures. According to the sedimentologically established age model derived in this study, the relocation of the river mouth resulted roughly in a doubling of the bulk sedimentation rates (including flood layers) from 1.8 and 0.8 cm year^{-1} to 3.6 and 1.2 cm year^{-1} in core 4 and core 5, respectively, which substantially contributed to the rapid growing of the prograding delta fan. It becomes clear that without any remedy measures, the remaining part of the northwestern bay of Lake Lauerz will be separated from the rest of the lake as an isolated pond in less than 200 years (Bussmann 2006).

Reconstructing regional palaeostorminess

We identified at least 54 and 68 flood layers (Lithotype B2) in core 1 and 3, respectively. To account for the difference

in sedimentation rates between the rapidly deposited flood layers and the comparably slow accumulation of the background sediment, we excluded the B2-layers from each of the two cores before creating age models. Moreover, constant sedimentation rates for the whole core and between successive fixed ages were assumed in core 3 and 1, respectively. The resulting flood event chronology reveals a major difference in the number of flood events that are recorded per 100 year between the two cores. A mean of 2.7 flood layers per 100 year are deposited in delta-distal core 1, whereas up to 28 flood layers occur within 100 year of sedimentation during the past 300 year in delta-proximal core 3. Presumably, this difference is caused by the smooth subaquatic ridge, which divides the western, delta-proximal basin from the eastern, delta-distal basin. Potentially, this ridge reduces significantly the sediment transport capability of density currents in addition to the normal decrease with increasing source-distance. However, one could argue that only major flood events are likely to deposit a B2-layer in the eastern basin, what makes this flood event record even more valuable for assessing the frequency of truly exceptional runoff events. Therefore, the subsequent reconstruction of outstanding rainfall events is based on core 1.

Within the past 2,000 years, we identified clearly three periods, in which the recurrence frequency of extreme storm-related floods was significantly high (Fig. 9). These evenly numbered intervals (II, IV, VI) are separated from each other by odd intervals (I, III, V, VII), in which almost no flood layers were deposited. The complete absence of flood layers within interval V could partly be attributed to the occurrence of coring disturbances at this particular

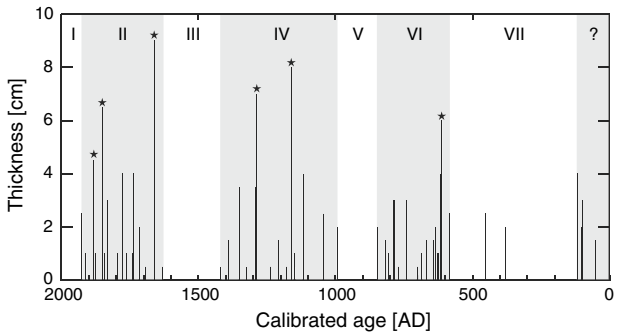

Fig. 9 Chronology of flood layers based on sedimentological recognition of 1806 AD event layer and additional ^{14}C ages from core 1. Individual layers were dated after removing thickness of B2- and B3-layers assuming constant sedimentation rates for individual intervals between adjacent datings. Even numbered, *shaded areas* represent periods with frequent occurring flood layers separated from each other by calm periods (*odd numbered*) with few to none flood events. Events marked with *stars* represent the six most outstanding layers, revealing thickness >4 cm. They are dated to 1876 (see text), 1850, 1660, 1290, 1160, and 610 AD, respectively, and are interpreted to represent runoff events with exceptionally high magnitudes

composite depth, which might inhibit the recognition of potentially existent B2-layers. The clusters of frequently occurring storms are dated to 1940–1630 AD (interval II), 1420–990 AD (interval IV), and 850–580 AD (interval VI), respectively, and exhibit an average recurrence interval of flood layers of 21.3 years.

The thickness of the flood layers deposited in core 1 ranges between 0.5 and 9 cm implying variations in the energy or size of density currents causing sediment transport and layer deposition. Such variations suggest time-dependent changes in storm size (Brown et al. 2000). By calibrating the most recent flood layer thickness using historical or even instrumental data, rough estimates of past storm magnitudes can be made (Brown et al. 2000). Zeller et al. (1978) provide instrumental precipitation data recorded at a meteorological station located on the upper course of the Steiner Aa (Sattel) for the period between 1901 and 1970 AD. In core 1, the topmost, 2.5-cm-thick flood layer (composite depth 57.0 cm; see Fig. 5) reveals an age (1926 AD), which is within age uncertainties consistent with the date of the largest flood (amount of precipitation within 24 and 48 h) occurring in the period of measurement in September of 1934 AD (slight discrepancy between the ages can be attributed to higher sedimentation rates due to lower compaction rates at the top of the core). As described beforehand, this exceptional hydrologic event resulted in a severe flood capable of rerouting the Steiner Aa in its delta. It was caused by a powerful storm, which led to severe devastation focused in the area around Lake Lauerz (Röthlisberger 1991).

If layer thickness is a proxy for the storm magnitude, as suggested by Brown et al. (2000), then 17 of the 54 events we identify in the basinal core 1 were larger than the 1934 AD flood pointing towards the occurrence of highly catastrophic runoff events in the past 2,000 years within the catchment of Lake Lauerz (Fig. 9). Six events are clearly standing out from the 17 layers since they show layer thickness of more than 4 cm. The first of them is 4.5 cm thick and exhibits an age (1883 AD) likely coinciding with the catastrophic flood event of 1876 AD, which was caused by the highest precipitation within the past 130 year (Pfister 1999). In the city of Zürich, located 35 km to the north of the catchment area in the Swiss Plateau, 430 mm of precipitation were registered, which corresponds to the highest amount of monthly rainfall ever recorded at this particular location. Moreover, the continuous rain was focused on Central and Eastern Switzerland (Pfister 1999) supporting the assumption that this layer can be attributed to the described exceptional runoff event. The five remaining outstanding storm events are dated to 1850, 1660, 1290, 1160, and 610 AD and are recorded as even thicker B2-layers underlining the remarkable magnitude of these events. However, to further establish the

palaeostorminess of Central Switzerland, additional archives should be considered since storm chronologies derived from single lakes can be susceptible to local environmental bias (Noren et al. 2002). Such bias includes the geologic character of the drainage basin, local differences in antecedent soil moisture or other factors of landscape conditioning, and core location, so that relationships between local events and wider climate patterns may not be revealed clearly by a single record (Noren et al. 2002). Nevertheless, the chronology of outstanding flood events established in this study represents an independent climate record, which reveals new and highly resolved data illustrating the regional climate history of the past 2,000 years.

The Rossberg landslide history

In order to track past mass wasting events occurring in the Rossberg area, both basinal cores were scanned for layers, which show similar sedimentological patterns as the 1806 AD-B3-layers described above. In core 3, which is located more proximal to the sedimentary source and to the area potentially affected by Rossberg landsliding events, remarkably high sedimentation rates delimit the use of this particular archive for the reconstruction of past mass wasting events, since the base of the core dates back only as far as 1700 AD. However, two layers exhibit sedimentological characteristics similar to those observed within the outstanding 1806 AD layer. They are located at 579–586 cm and below 789 cm, respectively, whereas the base of the deeper layer was not retrieved (bottom of core). The most conspicuous features are their relatively high TOC contents pointing towards an increased influx of organic matter during deposition yielding a brownish color of these layers. However, the thickness of the upper layer is significantly smaller (7 cm) as the thickness observed for the 1806 AD layer (32 cm), and coarse organic macroremains are missing. Moreover, assuming the same constant sedimentation rate as deduced for the last 200 years also for the pre-1806 interval, the layers are dating only as far back as 1770 and 1690 AD, leading to the assumption that associated potential events would have been reported in written chronicles if their impact on society was in the order of a major landslide. To explain the apparently high TOC contents, a scenario, which includes debris flow activity or minor shallow slides either in the area south of Lake Lauerz or around the course of the Steiner Aa during heavy rainfall seems to be the most likely explanation. The calculated ages for these two layers correlate within age uncertainties with the datings of two major flood-layers (1780 and 1660 AD) deposited in distal core 1, pointing towards increased runoff during time of deposition of the discussed strata. Considering all this, we interpret both layers to be flood layers, which potentially reflect the signal of increased small-scale mass wasting activity within the catchment area.

In core 1, we identified in addition to the 1806 AD layer one layer, which clearly can be attributed to a major landslide event. This layer is found at a composite depth of 578–598 cm and is visually unambiguously distinguishable from the frequently occurring B2-layers. A base containing coarse organic macroremains, probably reed plants, is the most remarkable feature of this prominent layer and leads to exceptional high TOC values of up to 7.6 wt%. A fining upward pattern is delimited at its top by a bright, albeit smeared cap. Density values reveal a significant minimum, which is reached by a decreasing downwards pattern similar to the one observed for the 1806 AD layer in the same core. Due to its outstanding thickness and the sedimentological, petrophysical, and chemical characteristics being highly similar to the ones described for the 1806-B3-layer, this layer is likely to represent the deposit created by a major landslide. By using the established age model, we derive a calibrated age of 810 ± 70 AD (2σ-range) for this event.

Only one additional major rockslide released from Rossberg is thought to have happened in historical times. Zay (1807) confirms the existence of a small village called ‘Röthen’, which was destroyed totally by the so-called Röthener rock avalanche before 1354 AD. Dettling (1860) suggests the year 1222 AD to be the date of the Röthener catastrophe, because based on archive studies, he claims the existence of a former village Röthen in 1220 AD. However, the assumed age is not well-constrained as written testimonies are lacking. Based on our data, we propose an approximate age of 810 ± 70 AD for this major mass wasting event, which is consistent with the age proposed by Zay (1807) but contradicts the age suggested by Dettling (1860). For this landslide, it is very likely that the release of the rock mass was associated with a catastrophic impulse wave comparable to the one observed in 1806 AD, because a huge amount of terrestrial material was relocated into the water body. Assuming an extent of Lake Lauerz even further to the west, a rock mass–water interaction, possibly identical or even stronger to the one described for the 1806 AD event is very likely because, although smaller in volume, the Röthener rock mass was released closer to the lake as the rock mass in 1806 AD (Fig. 1).

Next to this prominent B3-layer, five layers in core 1 reveal sedimentological characteristics, which are partially similar to both the 1806 AD and the 810 AD layer. Similar to core 3, they show TOC values that are significantly higher than observed in frequently occurring B2-layers. For the same reasons described above, we interpret these layers to be the product of exceptional rainfall events potentially in combination with small-scale mass wasting activity (e.g.

debris flows, shallow slides), which mobilized a higher amount of terrestrial organic matter as usually observed within B2 layers.

A reconstruction of the chronology of major rockfalls in the Rossberg area back to prehistoric times is impeded by remarkably high sedimentation rates observed in this highly clastic lake basin. Additional drilling within the frame of a larger project would probably be the key to overcome this problem providing a sedimentary record, which expands further back in time.

Conclusions

The analysis of four long piston cores containing the lacustrine succession deposited in Lake Lauerz during the past 2,000 years revealed the following main conclusions:

1. The catastrophic impulse wave observed in the course of the 1806 AD rock avalanche on Lake Lauerz was triggered by a sudden, gravity spreading-induced lateral displacement of a considerable amount of swamp deposits into the lake basin. This contradicts previous suggestions that the direct impact of the slide mass into the water body caused the devastating wave. The mobilization of the swampy material was the product of a mechanical failure of these deposits due to the rapid loading caused by the accumulating rock mass. As a consequence, we propose a conversion from an originally subaerial into a partially submerged landslide–water body interaction to be the ultimate trigger of the reported impulse waves. Such a process has furthermore implications on impulse-wave hazard assessments, since even shore-distal rockfalls may cause devastating water movements.
2. Basinal landslide event layers can be distinguished from flood layers on the basis of a higher TOC content caused by organic macroremains and by lower bulk-density values. A prominent mass movement-induced event layer is dated with 810 ± 70 AD and is proposed to represent the fingerprint of a major rock avalanche, the so-called Röthener Bergsturz. Based on our results, we suggest this mass-movement event to be substantially older than previously assumed.
3. The natural relocation of the Steiner Aa's river mouth during a exceptional rainfall event in 1934 AD is clearly identifiable in two cores from the modern delta area and resulted in a significant increase of sedimentation rate at these particular locations. This increase contributed substantially to the rapid growth of the actual prograding delta fan. We assume that without any remedy measures, the remaining part of the shallow northwestern bay of Lake Lauerz will be separated from the rest of the lake as an isolated pond in less than 200 years.
4. We identify three periods with clusters of frequently occurring flood events, which are dated to 580–850 AD, 990–1420 AD, and 1630–1940 AD, each revealing a mean recurrence interval of major flood layers of ~20 years. These periods are separated from each other by comparably calm periods, during which almost no flood layers were deposited.
5. Assuming flood layer thickness to be a proxy for the magnitude of a heavy rainfall, 17 events within the past 2,000 years are supposed to reveal runoff events of higher intensity as the heavy rainfall in 1934 AD pointing towards the occurrence of highly catastrophic flood events during the analyzed period. Within these 17 flood layers, 6 are outstanding in terms of layer thickness and are dated to approximately 610, 1160, 1290, 1660, 1850, and 1876 AD, respectively. The most recent one is representing a well-known flood event involving the highest amount of precipitation ever recorded in numerous regions of the Swiss Plateau (Pfister 1999).
6. Traces of prehistoric mass wasting events (e.g. the postulated 'Oberarther landslide') were beyond the reach of the coring techniques applied in this study. However, this pilot work points towards the ability of using lake sediments for reconstructing past landslide activity. Additional drilling would probably be the key to further establish the prehistoric chronology of the Rossberg's mass wasting succession.

Acknowledgments The authors would like to thank Robert Hoffmann for his tireless technical support and Urs Gerber for the outstanding quality of the core photographs presented in this paper. Emmanuel Chapron, Gaudenz Deplazes, Michael Strasser and Ingo Völksch assisted the field campaigns. We are indebted to the 'Naturforschende Gesellschaft Luzern' for financing the radiocarbon dating of the sediment and to Irka Hajdas for conducting these measurements. Michael Plötze kindly supported clay mineralogical analysis. Comments and suggestions of Frank Niessen and Kurosch Thuro significantly improved and completed the manuscript and are kindly acknowledged. The study was supported by the Swiss National Science Foundation.

References

Anselmetti, F. S., Ariztegui, D., Hodell, D. A., Hillesheim, M. B., Brenner, M., Gilli, A., et al. (2006). Late quaternary climate-induced lake level variations in Lake Petén Itza, Guatemala, inferred from seismic stratigraphic analysis. *Palaeogeography, Palaeoclimatology, Palaeoecology, 230*, 52–69.

AquaPlus (2002). Entwicklung des Gesamtphosphors im Lauerzersee anhand der im Sediment eingelagerten Kieselalgen. Unpublished report, Zug, 49 pp.

AquaPlus (2006). Ergänzungen zur Rekonstruktion der Trophiegeschichte und des Gesamtphosphors des Lauerzersees mittels im Sediment eingelagerten Kieselalgen. Unpublished report, Zug, 19 pp.

Bardet, J.-P., Synolakis, C. E., Davies, H. L., Imamura, F., & Okal, E. A. (2003). Landslide tsunamis: Recent findings and research directions. *Pure and Applied Geophysics, 160*, 1793–1809.

Becker, A., Ferry, M., Monecke, K., Schnellmann, M., & Giardini, D. (2005). Multiarchive paleoseismic record of late Pleistocene and Holocene strong earthquakes in Switzerland. *Tectonophysics, 400*, 153–177.

Berner, C. (2004). Der Bergsturz von Goldau: Geologie, Ausbreitung und Dynamik des grössten historischen Bergsturzes der Schweiz. Unpublished Diploma Thesis, ETH Zurich, 105 pp.

Brown, S. L., Bierman, P. R., Lini, A., & Southon, J. (2000). 10 000 yr record of extreme hydrologic events. *Geology, 28*(4), 335–338.

Büchi, U. P., & Amberg, R. (1983). Erdgasindikationen des schweizerischen Alpennordrandes. *Bulletin der Schweizerischen Vereinigung von Petroleum-Geologen und –Ingenieuren, 49*(117), 69–94.

Bussmann, F. (2006). The sediments of Lake Lauerz (Central Switzerland)—a new approach to establish the timing of the Rossberg landslide succession and the chronology of exceptional rainfall events. Unpublished Diploma Thesis, ETH Zurich, 82 pp.

Chapron, E., Desmet, M., De Putter, T., Loutre, M. F., Beck, C., & Deconinck, J. F. (2002). Climatic variability in the northwestern Alps, France, as evidenced by 600 years of terrigenous sedimentation in Lake Le Bourget. *The Holocene, 12*, 177–185.

Dettling, M. (1860). *Schwyzerische Chronik.* Schwyz: Triner.

Eden, D. N., & Page, M. J. (1998). Paleoclimatic implications of a storm erosion record from late Holocene lake sediments. *Palaeogeography, Palaeoclimatology, Palaeoecology, 139*, 37–58.

Fritz, H.M. (2002). Initial phase of landslide generated impulse waves. Mitteilungen der Versuchsanstalt fürWasserbau, Hydrologie und Glaziologie 178. ETH Zurich, 254 pp.

Fritz, H. M., Hager, W. H., & Minor, H.-E. (2001). Lituya Bay case: Rockslide impact and wave run-up. *Science of Tsunami Hazards, 19*(1), 3–22.

Fritz, H. M., Hager, W. H., & Minor, H.-E. (2004). Near field characteristics of landslide generated impulse waves. *Journal of Waterway, Port, Coastal and Ocean Engineering, 130*(6), 287–302.

Gasser, J. (2003). 200 Millionen Jahre Erdgeschichte. *Berichte der Schwyzerischen Naturforschenden Gesellschaft, 14*, 63–82.

Gilli, A., Anselmetti, F. S., Ariztegui, D., & McKenzie, J. A. (2003). A 600-year sedimentary record of flood events from two subalpine lakes (Schwendiseen, Northeastern Switzerland). *Eclogae Geologicae Helvetiae, 96*(Suppl 1), 49–58.

Gilli, A., Ariztegui, D., Anselmetti, F. S., McKenzie, J. A., Markgraf, V., Hajdas, I., et al. (2005). Mid-Holocene strengthening of the Southern Westerlies in South America—Sedimentological evidences from Lago Cardiel, Argentina (49°S). *Global and Planetary Change, 49*, 75–93.

Giovanoli, F., Kelts, K., Finckh, P. & Hsü, K.J. (1984). Geological framework, site survey and seismic stratigraphy. In Quaternary geology of Lake Zurich: An interdisciplinary investigation by deep-lake drilling. Contributions to Sedimentology, vol. 13, pp 5–20.

Hantke, R. (2006). *Blatt 1151 Rigi, mit Nordteil von Blatt 1171 Beckenried. Geologischer Atlas der Schweiz 1:25 000, Karte 116*. Wabern: Bundesamt für Landestopographie.

Heim, A. (1932). *Bergsturz und Menschenleben. Beiblatt zur Vierteljahrsschrift der Naturforschenden Gesellschaft in Zürich* (p. 218). Zürich: Beer & Co.

Kopp, J. (1936). Die Bergstürze des Rossberges. *Eclogae Geologicae Helvetiae, 29*(2), 490–493.

Kopp, J. (1960). Alte Flussläufe der Muota und Steiner Aa zwischen Rigi und Rossberg. *Eclogae Geologicae Helvetiae, 53*(2), 517–519.

Lambert, A., & Pfeiffer, C. (1990). Neuvermessung des Lauerzerseebeckens: Veränderungen des Seegrundes von 1892 bis 1989. *Wasser, Energie, Luft, 35*(9), 190–194.

Last, W. M. (2001). Mineralogical analysis of lake sediments. In W. M. Last & J. P. Smol (Eds.), *Tracking environmental change using lake sediments. Physical and geochemical methods* (Vol. 2). Dordrecht: Kluwer Academic Publishers.

Leemann, A. (1993). Rhythmite in alpinen Vorgletscherseen: Warvenstratigraphie und Aufzeichnung von Klimaveränderungen. Unpublished PhD Thesis, ETH Zurich, 129 pp.

Lehmann, O. (1942). Über Böschungswinkel und Böschungshöhen im Hinblick auf den Bergsturz von Goldau. *Eclogae Geologicae Helvetiae, 35*(1), 55–65.

Nadim, F., Kjekstad, O., Peduzzi, P., Herold, C., & Jaedicke, C. (2006). Global landslide and avalanche hotspots. *Landslides, 3*, 159–173.

Niessen, F. (1987). Sedimentologische, geophysikalische und geochemische Untersuchungen zur Entstehung und Ablagerungsgeschichte des Luganersees (Schweiz). Unpublished PhD Thesis, ETH Zurich, 332 pp.

Noren, A. J., Bierman, P. R., Steig, E. J., Lini, A., & Southon, J. (2002). Millenial-scale storminess variability in the northeastern United States during the Holocene epoch. *Nature, 419*, 821–824.

Pfister, C. (1999). *Wetternachhersage: 500 Jahre Klimavariationen und Naturkatastrophen* (p. 304). Bern: Paul Haupt.

Reimer, P. J., Baillie, M. G. L., Bard, E., Bayliss, A., Beck, J. W., Bertrand, C. J. H., et al. (2004). IntCal04 terrestrial radiocarbon age calibration, 0–26 Cal Kyr BP. *Radiocarbon, 46*(3), 1029–1058.

Röthlisberger, G. (1991). Chronik der Unwetterschäden in der Schweiz. Berichte der Eidgenössischen Forschungsanstalt für Wald, Schnee und Landschaft 330. Zurich, 122 pp.

Schneider, J.-L., Pollet, N., Chapron, E., Wessels, M., & Wassmer, P. (2004). Signature of Rhine valley sturzstrom dam failures in Holocene sediments of Lake Constance, Germany. *Sedimentary Geology, 169*, 75–91.

Schnellmann, M., Anselmetti, F. S., Giardini, D., & McKenzie, J. A. (2005). Mass movement-induced fold-and-thrust belt structures in unconsolidated sediments in Lake Lucerne (Switzerland). *Sedimentology, 52*, 271–289.

Schnellmann, M., Anselmetti, F. S., Giardini, D., McKenzie, J. A., & Ward, S. N. (2002). Prehistoric earthquake history revealed by lacustrine slump deposits. *Geology, 30*(12), 1131–1134.

Sletten, K., Blikra, L. H., Ballantyne, C. K., Nesje, A., & Dahl, S. O. (2003). Holocene debris flows recognized in a lacustrine sedimentary succession: Sedimentology, chronostratigraphy and cause of triggering. *The Holocene, 13*(6), 907–920.

Strasser, M., Anselmetti, F. S., Fäh, D., Giardini, D., & Schnellmann, M. (2006). Magnitudes and source areas of large prehistoric northern Alpine earthquakes revealed by slope failures in lakes. *Geology, 34*(12), 1005–1008.

Stuiver, M., & Reimer, P. J. (1993). Extended 14C database and revised CALIB radiocarbon calibration program. *Radiocarbon, 35*, 215–230.

Stuiver, M., Reimer, P. J., Bard, E., Beck, J. W., Burr, G. S., Hughen, K. A., et al. (1998). INTCAL98 radiocarbon age Calibration, 24000–0 cal BP. *Radiocarbon, 40*(3), 1041–1083.

Thuro, K., Berner, C., & Eberhardt, E. (2006). Der Bergsturz von Goldau 1806–200 Jahre nach dem Ereignis. *Felsbau, 24*(3), 59–66.

Trümpy, R. (1980). *Geology of Switzerland, a guide-book; Part A: An outline of the geology of Switzerland* (p. 104). Basel: Wepf & Co.

Vischer, D. L., & Hager, W. H. (1998). *Dam hydraulics* (p. 316). Chichester: Wiley.

Zay, K. (1807). Goldau und seine Gegend: wie sie war und was sie geworden. Orell, Füssli und Compagnie, Zürich, 390 pp.

Zehnder, J. (1988). Der Goldauer Bergsturz: Seine Zeit und sein Niederschlag. Verlag Stiftung Bergsturzmuseum Goldau, Goldau, 271 pp.

Zeller, J., Geiger, H., & Röthlisberger, G. (1978). *Starkniederschläge des schweizerischen Alpen- und Alpenrandgebietes (Volume 3); Intensitäten und Häufigkeiten; Ausgewertete Periode 1901–1970*. Birmensdorf: Eidgenössische Anstalt für das forstliche Versuchswesen.